공학석사 학위논문

# Assessment of Shear Band Characteristics in Cohesive Soils using Plane Strain Test with Digital Image Analysis

## 평면변형률 시험에서 디지털 이미지 해석을 통한 점성토에서의 전단면 특성 평가

**2014년 2월**

서울대학교 대학원

건설환경 공학부

곽 태 영

# Assessment of Shear Band Characteristics in Cohesive Soils using Plane Strain Test with Digital Image Analysis

## 평면변형률 시험에서 디지털 이미지 해석을 통한 점성토에서의 전단면 특성 평가

지도 교수 정 충 기

이 논문을 공학석사 학위논문으로 제출함

**2014년 2월**

서울대학교 대학원

건설환경공학부

곽 태 영

곽태영 석사 학위논문을 인준함

**2014년 2월**

위 원 장 _____ (인)

부위원장 _____ (인)

위 원 _____ (인)

# Abstract

## Assessment of Shear Band Characteristics in Cohesive Soils using Plane Strain Test with Digital Image Analysis

Kwak, Tae Young

Department of Civil and Environmental Engineering

The Graduate School

Seoul National University

Soil failure which affects the stability and deformation characteristics of structures is relevant to settlement by consolidation, and shear banding, the localization of deformation into thin zones. However, most of the existing researches for plane strain tests were performed with granular soils to evaluate those spatial deformations. Little research has been conducted with cohesive soils; even the existing research has no regard to spatial deformation, only considering the entire deformation which is measured by the conventional method (LVDT). Moreover, cohesive soils show significant heterogeneous deformation behaviors due to the non-uniform distribution of stress. Accordingly, the understanding of the characteristics of spatial deformation during consolidation and shear process is necessary as well as the assessment of stress-strain response of the soil. In this paper, digital image analysis technique with the advantage of high resolution for deformation at any point of a soil was adopted to evaluate the consolidation behavior and shear band characteristics of normally consolidated clays. Overall stress-strain behavior from initial to post peak has been analyzed

together with spatial distributions of deformations from digital images at 5 distinct loading intervals. Failure mechanism and strain softening is strongly related to the shear band forming and evolution.

**Keywords: Plane strain test, Digital image analysis, Strain distribution, Deformation condition**

**Student Number: 2012-20891**

# Contents

# List of Tables

# List of Figures

# Chapter 1 Introduction

## 1.1 General

Soil failure in slopes, foundations and retaining structures is initiated and preceded by forming and progressing of shear band, defined as the localization of deformation into thin zones of soil mass. This strain localization has a quite relevance, as stability and deformation characteristics of earth structures can be evaluated by the soil behavior in local parts where the deformation is concentrated (Desreus and Viggiani, 2004). However, the localization of deformation within cohesive soils shows a significant non-uniform distribution due to distribution of stress (Rhee, 1991). For this reason, assessment of deformation behavior of cohesive soils needs to be performed by understanding the strength and overall stress-strain behavior. In addition spatial deformation characteristics of an overall specimen from initial state to post-failure state need to be investigated.

Plane strain test was performed for two reasons. The first purpose is to simulate the plane strain (PS) condition. PS condition simulates the geotechnical constructions such as slope, shallow footing, embankment, or retaining structure, and overall behavior under PS condition shows significantly difference from triaxial condition (TX). (Lee, 1970; Marachi et al., 1981, Peters et al., 1988)

The second purpose is to observe the localization of deformation such as shear band characteristics. Internal deformation under PS condition

during shear shows the failure of specimen clearer than TX condition. Cylindrical specimen, which is used for TX test, has disadvantage to observing internal deformation. For the observation of internal deformation in the TX test, X-ray Computed Tomography (CT) was applied to scan the density variation (Mokni 1992; Desreus et al., 1996; Wong, 2000; Alshibli et al., 2003). Also epoxy impregnation in soil specimen was applied to analyze the thin section of the specimen (Kuo and Frost, 1996; Alshibli and Sture, 1999; Jang and Frost, 2000). However CT technique requires complicated scanner which is expensive, and also it cannot measure movement and deformation of soils during the test procedure. For this reason, it can be used just after the end of the test. Also epoxy impregnation method can investigate the void ratio and soil fabric after completing after test. In plane strain test, the rectangular parallelpiped specimen is used for the test, so the deformation behavior can be observed on a restrained plane. Therefore the internal deformation is easily investigated by using a transparent side wall for the plane strain test. Additionally, the deformation and failure pattern during shearing procedure under PS condition is different from TX condition. The failure mode under TX condition is complex conical shear plane. However, in the PS test the failure mode of specimen always occurs along a shear band. Therefore, the general failure mode can be more clearly simulated under PS condition rather than TX condition (Alshibli et al, 2003). In this study, plane strain tests were performed to focusing on observation of the spatial deformation in overall soil specimen during shearing.

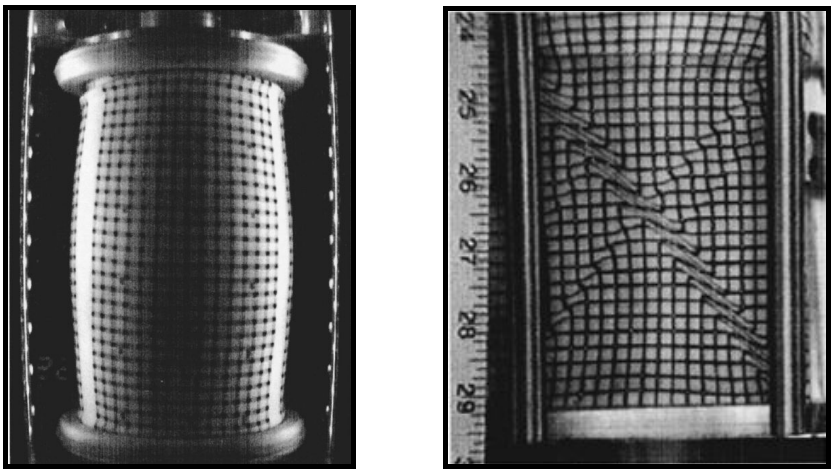


Fig. 1.1 Plane strain versus triaxial test (Alshibli et al., 2003)

The analysis of specimen deformation in the PS test was performed by application of the digital image analysis. Traditional method which uses measuring instrument like linear variable differential transformer (LVDT) or strain guage has difficulty in the evaluation of spatial deformation of the specimen. For observation of spatial deformation, two consecutive images captured at different times through the transparent side wall were used for the digital image analysis method. Existing methods for evaluation of internal deformation were performed by tracing reference markers or grid points on membrane which cover the specimen (Desreus, 1984; Liang et al., 1997; Alshibli and Sture, 2000). However the method by reference markers cannot investigate the overall internal deformation, it just can investigate the internal deformation at few points. Recently, the automated digital image analysis methods have been utilized to enable accurate displacement measurements and perform analysis for large amount of data (White et al., 2003). By

automated digital image analysis method, spatial deformation on specimen under PS condition can be evaluated. However the accuracy of automated digital image analysis for cohesive soils has not been verified under various conditions. In this paper, the optimal analysis condition for cohesive soils will be suggested and it will be applied to assessment of shear band characteristics.

## 1.2 Aim and Scope of Study

The main purpose of this study is evaluation of the shear band localization for cohesive soils under PS condition. For the evaluation of the shear band localization, it will be divided into two parts. The first is the experimental investigation of shearing behavior by the plane strain tests. The second is the digital image analysis by the images which was captured during the shearing of the cohesive soils.

*Experimental Study*

The plane strain tests using digital image analysis were performed to investigate internal deformation localization. Firstly, two vertical compression tests were performed; normally consolidated clay (NC) and overconsolidated clay (OC). Stress-strain behavior of these two clays during the shearing procedure of cohesive soils is analyzed with the acquisition of digital images. Secondly, digital image analysis method is adopted to investigate the internal deformation of cohesive soils. The displacements were measured via an optimal digital image analysis, and strains of a defined unit element were evaluated from displacement field. Finally, the spatial deformation of specimen is evaluated during the occurrence and development of a shear band during the shearing procedure.

## 1.3 Outline

This study is divided into five chapters.

Chapter 2 provides experimental background of plane strain test and digital image analysis. The existing plane strain testing apparatus is explained with some examples and digital image analysis method is also explained.

Chapter 3 describes the experimental program about plane strain test with developed plane strain testing apparatus and verification of digital image analysis method for cohesive soils. In addition detail procedures including test system, specimen, and condition are explained.

Chapter 4 presents the experimental results for plane strain test with digital image analysis method. Internal deformation localization difference for NC clay and OC clay is compared.

Chapter 5 summarizes the results by deformation behavior with stress-strain behavior and presents its conclusion.

# Chapter 2 Background

## 2.1 Background of the Plane Strain Test

### 2.1.1 Conventional Testing Apparatus

For simulating PS condition experimental tests require a restraint of deformation in one horizontal direction. Many researchers have developed various testing apparatus which uses rectangular parallel piped specimen.

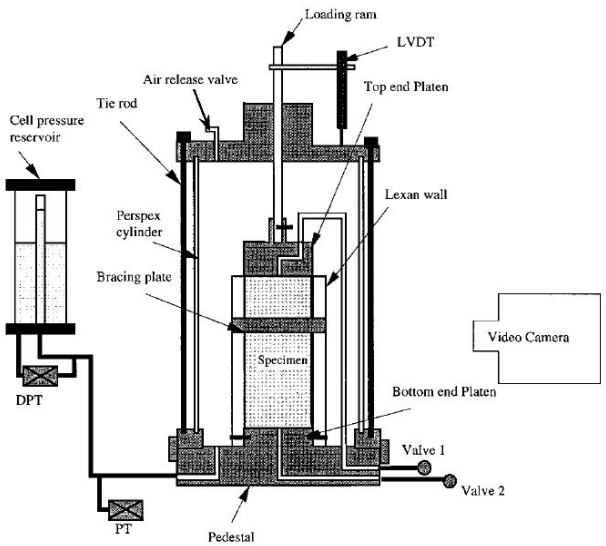


Fig. 2.1 Conventional PST apparatus (Alshibli and Sture, 1999)

Figure 2.1 is the schematic diagram of the general conventional plane strain testing apparatus. Plane strain testing apparatus is similar to the conventional triaxial testing apparatus. Cylindrical cell is used to withstand against confining stress. And the specimen is wrapped with the membrane, and it is restrained by two side walls to simulate PS condition. Two side walls are braced for the complete fixing of them and vertical movement of the rod. One of the side walls is transparent rigid wall which can be captured by video camera. Two drainage lines (valve 1 and valve 2) also installed on the upper and lower part of specimen to measure the volume change and pore pressure. In addition loading ram for vertical load is set at upper plate of the testing apparatus.

However there are some limitations on the general plane strain testing apparatus. First is the restrained bottom plate because of difficulties in manufacturing the equipment. Plane strain test with restrained bottom plate makes a difference from field condition because of shear stress on bottom plate. Second is the gap between the specimen and side walls because of no equipment between side walls and specimen. Cell water can infiltrate into the gap, and this phenomenon may cause the destruction of PS condition.

### 2.1.2 Advanced Testing Apparatus

To overcome the limitations of the conventional testing apparatus, some testing apparatus have been developed. Figure 2.2 shows the first advanced testing apparatus which adopted unrestrained bottom plate. This sliding system by adopting restrained bottom plate allows free lateral displacement which enables minimizing the shear stress acting on the end plates. Therefore shear band can be developed with the best geometric configuration for optical measurement. This system simulates the failure condition of the geotechnical field.

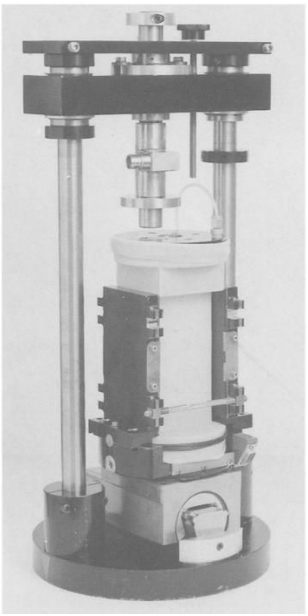

Fig. 2.2 Advanced plane strain testing apparatus with unrestrained bottom plate (Drecher et al., 1990)

The second advanced testing apparatus is the system with wall stress measurement by local gauge. The local measurements for localized deformation and stresses by transducers have been installed in the pressure cell of plane strain testing apparatus. It is illustrated in Figure 2.3

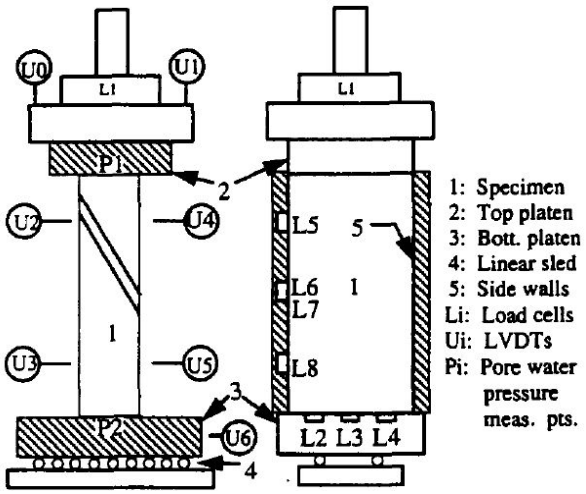


Fig. 2.3 Advanced plane strain testing apparatus with local gauges (Finno et al., 1996)

The third advanced testing apparatus is developed by Kim et al. (2006) to simulate the various stress path tests. The apparatus illustrated in Figure 2.4 adopted a membrane that wraps both the specimen and the walls to prevent water infiltration between specimen and the side walls. This system can maintain the plane strain condition.

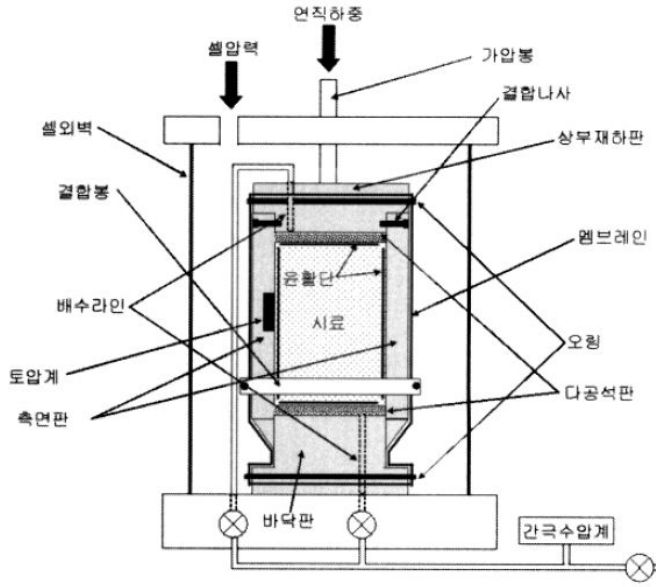


Fig. 2.4 Advanced plane strain testing apparatus for various stress paths (Kim et al., 2006)

## 2.2 Background of the Digital Image Analysis

Conventional method as explained in Chapter 1, particular tools such as LVDT or strain guage have some limitations. These measurement devices have difficulty in observing deformation at various spatial points. In addition, X-ray computed tomography and epoxy injection methods have several limitations as mentioned at introduction. For these reasons, the automated digital image analysis methods have been widely used to measure displacements and deformation of the object.

There are some necessary conditions for digital image analysis; 1) object for investigation which should be deform in the plane, 2) camera direction that must be perpendicular with the plane of the object, 3) uniform lighting for illuminator. Therefore some research for plane strain test adopted digital image analysis methods satisfying these requirements (Rechenmacher et al., 2004, Jang et al., 2008). There are two categories for digital image analysis methods; first is particle image velocimetry (PIV) and the other is digital image correlation (DIC). In this study, PIV technique is adopted for analysis.

### 2.2.1 Concept of Particle Image Velocimetry (PIV)

Particle image velocimetry (PIV) technique was developed for measuring the displacement and velocity of a moving material in fluid mechanics (Adrian, 1991). PIV technique for geotechnical engineering was developed to measure the displacement between a pair of digital images (White et al., 2003). Processes for PIV technique are explained below:

(1) Images are divided into a grid of patches.

(2) Tested patches are selected in a pre-deformed image.

. (3) Estimated moving range of each grid of patches is determined with an expected displacement in a deformed image.

(4) The displacement vector of each patches during the interval between the flashes are found by locating the peak of the auto correlation function of each patch.

The cross-correlation between the grid of patches between pre-deformed image and deformed image is calculated by Equation 2.1 and procedure is illustrated at Figure 2.5.

$$C = \frac{\sum [F \bullet G]}{(\sum F^2 \times \sum G^2)^{1/2}} \qquad (2.1)$$

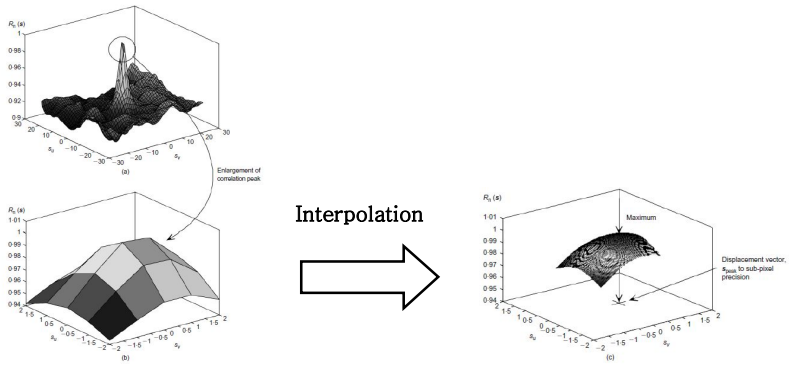


Fig. 2.5 Cross-correlation procedure in PIV technique (White et al., 2003)

## 2.2.2 Influence Factors for PIV Technique

There are several influence factors which influence to the accuracy and precision of soil deformation. Influence factors for PIV technique is listed below:

(1) Image resolution

(2) Size of pixel subset

(3) Image pattern

(4) Deformation condition

*Image resolution*

Image resolution expressed by unit of mm/pixel is determined by the capacity and range of digital camera. As capacity of digital camera becomes higher and range of image capture becomes narrow, image with high resolution can be acquired. Figure 2.6 shows the image resolution by capacity and range of digital camera.

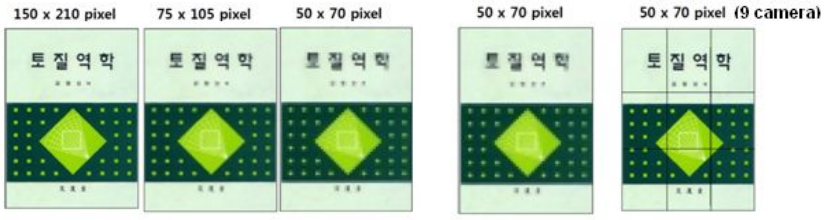


Fig. 2.6 Image resolution by capacity and range of digital camera

*Size of pixel subset*

For the measurement of displacement by digital image methods pixel subset is used for uniqueness of image pattern to guarantee the correlation between images. Generally as pixel subset becomes larger, the accuracy and precision of result of digital image analysis method becomes higher. However huge size of pixel subset has limitation in measuring the various spatial deformations. Therefore adequate size of pixel subset should be selected prior to the test.

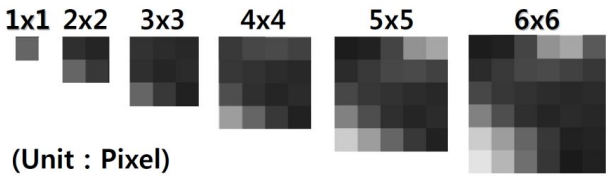


Fig. 2.7 Image pattern by size of pixel subset

*Image pattern*

For digital image analysis, images should be constituted by various values of grey level. Image pattern with various values of grey level can reach to accurate analysis result by distinct correlation peak. High uniqueness of image pattern results in high accuracy of analysis. Each particle of granular soils has various colors, and it enables accurate digital image analysis. However cohesive soils have limitations for accurate digital image analysis, because cohesive soils are constituted with particle of uniform color. For this reason, arbitrary pattern should be prepared by spray ink or mixed by flame-colored granular soil.

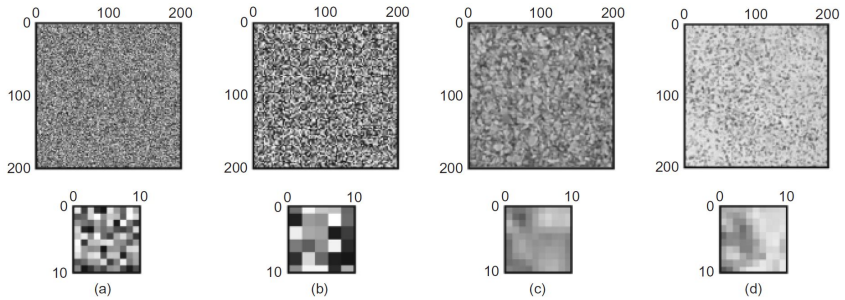


Fig. 2.8 Image pattern used for PIV validation test:
(a) random image; (b) random image, 2 x 2 ‘grains’; (c) Dog`s Bay sand;
(d) kaolin clay with artificial texture (White el al., 2003)

*Deformation condition*

Deformation of soil specimen can be divided into three categories; one is rigid body translation, another is compression and tension, and the other is shear deformation. In digital image analysis, rigid body translation can reach to accurate analysis results. However actual specimen includes not only rigid body translation, but also compression, tension and shear deformation. Because of these deformation conditions, verification of adequate deformation condition is necessary. Especially when degree of deformation is too large, standard error of analysis results becomes larger. For this reason, estimation of threshold strain by evaluation of accuracy is needed with adequate interval of image capture.

# Chapter 3 Experimental Program

## 3.1 Introduction

Plane strain tests and digital image analysis are adopted for the experimnetal study in this paper. In this chapter, experimental procedure using planes strain tests and digital image analysis is defined prior to the experimental analysis. Vertical compression tests on two soil conditions; normally consolidated (NC) clay and overconsolidated (OC) clay; were conduted with capturing digital images by using a developted plane strain testing apparatus. In addition the images captured at different times, displacements at various points were computed by the GeoPIV which is developed digital image analysis technique software (White et al., 2003). Also engineering strains of defined unit elements were evaluated from the displacement field.

## 3.2 Developed Plane Strain Testing Apparatus

Newly developed plane strain testing apparatus is illustrated in Figure 3.1 (Jang, 2010). Rectengular soil specimen, 128mm in height, 65mm in width and 45mm in length, is used for a plane strain tests. Its ratio of the diameter to height is approximately 0.5, which is generally adopted in triaxial tests. Two rigid side walls connected with fixed fedestal are applied to restrain the axial deformation in one direction. The lower parts of the walls are fixed with the bottom plate which can control the restrain condition.

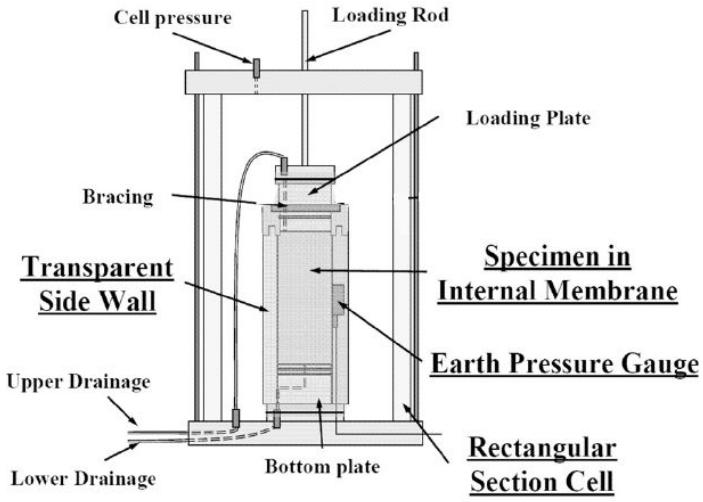


Fig. 3.1 Newly developed plane strain testing apparatus (Jang, 2010)

*Side walls*

Two rigid walls which is shown in Figure 3.2 restrain the deformation of one axial deformation. One side wall is made of acrlyic in order to capture the images. Acrylic transparent wall is used for evaluation of deformation characteristics of the soil specimen. The upper parts of side walls are fixed by bracing in order to restrain the relative displacement of the side walls and confirm the verticality of the rod. In addition vacuum grease is used for the contact between soil specimen and side walls to reduce the wall friction.

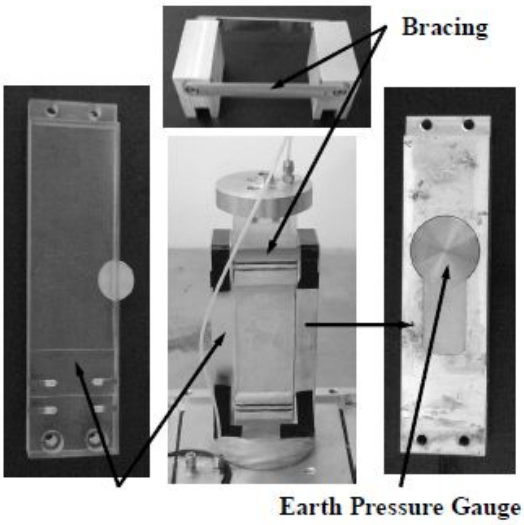


Fig. 3.2 Side walls used for plane strain test (Jang, 2010)

*Unrestrained bottom plate*

Bottom plate is mainly composed of two mechanical parts. A lower part of bottom plate is fixed on the pedestal, and upper plate can be move freely for axial direction. System of unrestrained bottom plate is illustrated at Figure 3.3. The linear bearing is installed between the fixed bottom plate and the movable bottom plate to reduce the friction. This system enable to prevent the shear stress acting on end of the soil specimen where the specimen is contact with bottom plate.

While the specimen is prepared and consolidated, the movable bottom plate is restrained by the inserting four of small rods at the base of the movable bottom plate. To allow lateral movement of the bottom plate during the shearing, four of small rods are lowered from the movable bottom plate. This mechanical composition allowed for more efficient conditions to track the generation of a shear band by minimizing the friction on the bottom plate (Alshibli et al., 2004; Finno et al., 1997; Jang et al., 2008).

Fig. 3.3 Unrestrained bottom plate (Jang, 2010)

*Pressure cell box*

Cylindrical cells were mostly used for triaxial test to prevent stress concentration. Its shape maintain the safety of the cells because of the preventability of stress concentraion. However, the shape of pressure cell disturb the image capturing from the outside of the cell by the refraction and distortion. To overcome the limitations of cylindrical cell, rectangular pressure cell is used for capturing undistorted digital images as illustrated in Figure 3.4.

Fig. 3.4 Rectangular pressure cell (Jang, 2010)

*Testing system*

Plane strain tests are performed with the C.K.C loading frame, which is conventionally used for the loading system. The testing system is composed of load cell, LVDT, and the pressure transducer. The strain is calculated by the displacement which is measured by LVDT, and the stress is measured by the load cell. In addition, lighting is used for constant brightness during the plane strain tests to capture the images. Its system is shown in figure 3.5 and 3.6.

Fig. 3.5 C.K.C loading frame

Fig. 3.6 Lighting for constant brightness

## 3.3 Digital Image Analysis for Cohesive Soils

Digital image analysis methods should be evaluated under various conditions for assessment of soil deformation. For this reason, digital image analysis methods were verified at some researches by comparison between digital image analysis results and practical results of testing specimen (White et al., 2003; Rechenmacher and Finno., 2004; Jang et al., 2008). However, most of these researches did not consider the influence factor which is explained at Chapter 2.

In this chapter, the digital image analysis condition for cohesive soils is verified by GeoPIV which is developed by White et al. (2003). The deformation of the soil specimen analyzed by captured images during the plane strain tests. And then, the results analyzed by digital image analysis methods were compared with the actual deformation measured by LVDT. In addition digital image analysis method conditions for cohesive soils are suggested.

### 3.3.1 Verification of Digital Image Analysis (GeoPIV)

To verify the accuracy of digital image analysis method, the results by GeoPIV which is developed by White et al. (2003) are compared to the exact displacements. The difference between analyzed results and exact displacements are compared by the standard error concept depicted in equation 3.2. The standard error is calculated by using $u_{dia}$, $v_{dia}$ from the digital image analysis and $u_{exact}$, $v_{exact}$ from the exact results.

$$\text{Std\_Err} = \sqrt{\frac{\sum_{i}^{n}[(u_{DIA} - u_{EXACT})^2 + (v_{DIA} - v_{EXACT})^2]}{N}} \qquad (3.1)$$

The accuracy of GeoPIV is verified by two images; the first image is the initial image and the other is the image which is moved by rigid body motion. The errors are computed by various pixel subsets; 40 by 40, 60 by 60, 80 by 80, 100 by 100, and 120 by 120 pixels. In addition the errors are computed by two deformation condition; 1pixel rigid body motion and 10 pixel rigid body motion. The results of verification of GeoPIV are shown in Table 3.1 and 3.2.

Table 3.1 Standard errors at 1 pixel rigid body motion

| Pixel subset | Accuracy | | Precision | |
|---|---|---|---|---|
| | Horizontal | Vertical | Horizontal | Vertical |
| **40 by 40** | 0.1860 | 0.2131 | 0.3223 | 0.3580 |
| **60 by 60** | 0.1017 | 0.1154 | 0.1349 | 0.1613 |
| **80 by 80** | 0.0626 | 0.0830 | 0.0834 | 0.1133 |
| **100 by 100** | 0.0557 | 0.0575 | 0.0682 | 0.0765 |
| **120 by 120** | 0.0451 | 0.0501 | 0.0526 | 0.0647 |

Table 3.2 Standard errors at 10 pixel rigid body motion

| Pixel subset | Accuracy | | Precision | |
|---|---|---|---|---|
| | Horizontal | Vertical | Horizontal | Vertical |
| **40 by 40** | 0.1918 | 0.2032 | 0.2909 | 0.3518 |
| **60 by 60** | 0.1063 | 0.1132 | 0.1492 | 0.1985 |
| **80 by 80** | 0.0705 | 0.0861 | 0.0903 | 0.1209 |
| **100 by 100** | 0.0576 | 0.0590 | 0.0695 | 0.0764 |
| **120 by 120** | 0.0441 | 0.0572 | 0.0525 | 0.0830 |

## 3.4 Test & Analysis Procedure

### 3.4.1 Test specimen

EPK kaolinite which represents the cohesive soils was used for plane strain test. The index properties of reconstituted kaolinite are summarized in Table 3.3. In addition the images of test specimen are shown in Figure 3.7.

Table 3.3 Properties of reconstituted kaolinite

| Liquid limit | Plastic index | Specific gravity | USCS | E0 | Water content |
|---|---|---|---|---|---|
| 65.3% | 23.1% | 2.62 | MH | 1.60 | 61.0% |

Fig. 3.7 Reconstituted kaolinite

*Trimming device*

To prepare the rectangular specimen for granular soils, the rectangular mold is used. However cohesive soils need trimming for rectangular specimen. For this reason trimming device is manufactured. Procedure of trimming device is shown in Figure 3.8. Rectangular cohesive soils are shown in Figure 3.9.

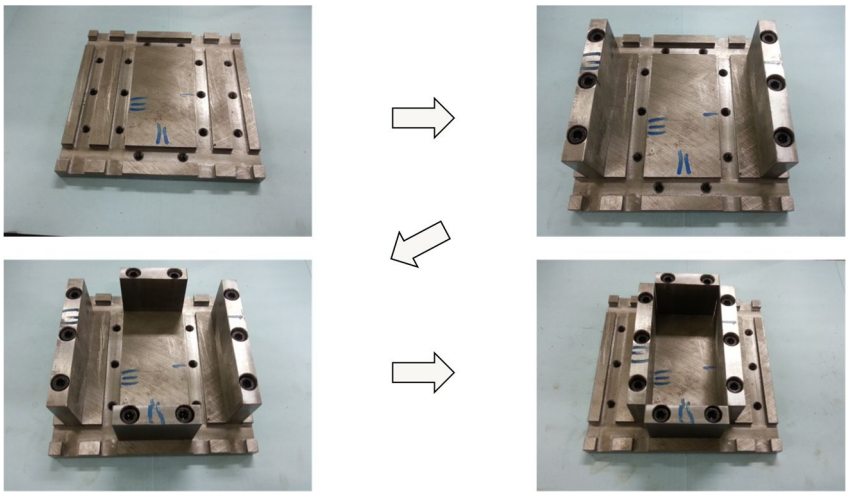

Fig. 3.8 Procedure of trimming device

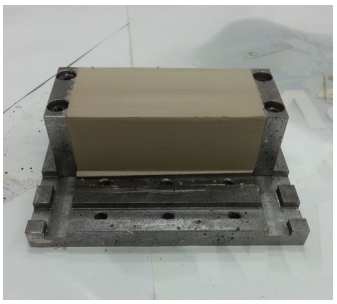

Fig. 3.9 Soil specimen for plane strain test

*Image pattern*

For digital image analysis, movement of soil particles is analyzed for granular soils. Each particle of granular soils has different colors which guarantee the uniqueness of pixel subset. However each particle of cohesive soils has uniform color, which has difficulty in digital image analysis. For this reason image pattern for cohesive soils is needed. For the arbitrary image pattern for cohesive soils spray ink is used (Kim et al., 2008). The arbitrary pattern by spray ink which guarantees the uniqueness of pixel subset is shown in Figure 3.10.

Fig. 3.10 Image pattern for cohesive soils (Kim et al., 2008)

### 3.4.2 Test Conditions

Two consolidation conditions are adopted for plane strain test; shearing behavior of normally consolidated (NC) soils and over-consolidated (OC) soils is compared. Both of consolidation conditions are firstly consolidated by 230kPa of effective vertical pressure with 140kPa of effective confining pressure. Then NC soils are performed shearing directly after the consolidation. OC soils consolidated same as normally consolation soils for loading procedure. However for OC condition, unloading should be adopted; 55kPa of effective vertical pressure with 55kPa of effective confining pressure. These two conditions adopted $K_0$ consolidation concept which is depicted in Equation 3.2. In addition test conditions are summarized in Table 3.4.

$$K_0 = (1-\sin\phi)(OCR)^{\sin\phi} \Rightarrow For\ \ OCR = 4,\ K_0 \approx 1 \qquad (3.2)$$

Table 3.4 Test conditions for plane strain test

| | **NC clay** | | **OC clay** | |
|---|---|---|---|---|
| | **Vertical stress ($\sigma_1$')** | **Horizontal stress ($\sigma_3$')** | **Vertical stress ($\sigma_1$')** | **Horizontal stress ($\sigma_3$')** |
| **Loading** | 230kPa | 140kPa | 230kPa | 140kPa |
| **Unloading** | - | - | 55kPa | 55kPa |

### 3.4.3 Test & Analysis Procedure

After specimen preparation, plane strain test is performed with acquisition of digital images. Stress-strain behavior can be measured by plane strain test and deformation characteristics can be evaluated by digital image analysis. Procedure diagram is shown in Figure 3.11.

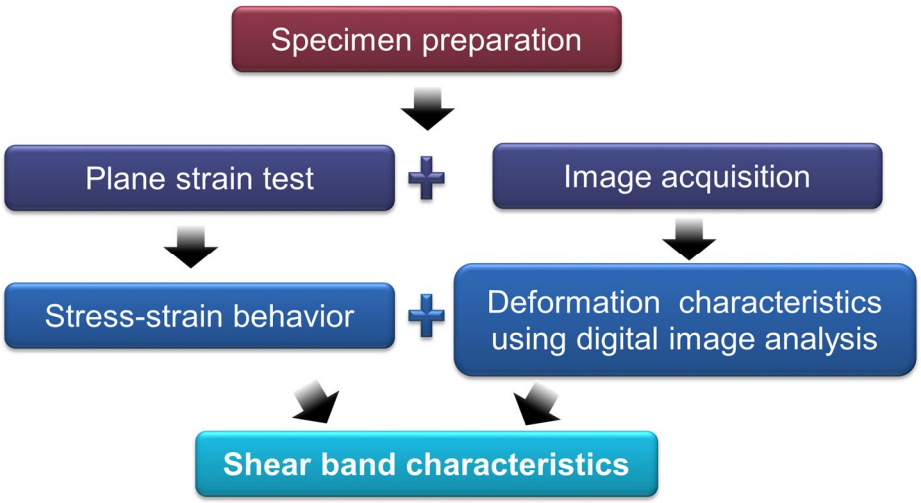


Fig. 3.11 Procedure diagram of test & analysis procedure

*Test procedure*

Under plane strain conditions with restrained bottom plates, the specimen is axially compressed until the stress-strain response exhibited the residual state. Unrestrained bottom plate condition can simulate the failure condition of field. During compression, sequential digital images of the transparent wall were taken by high-resolution digital camera (Nikkon D90).

*Analysis procedure*

To analyze the deformation characteristics from initial to post-failure state, five stages were selected from stress-strain behavior as illustrated in Figure 3.12; 1) initial stage, 2) peak stage, 3) softening stage, 4) steady state, 5) post-failure stage.

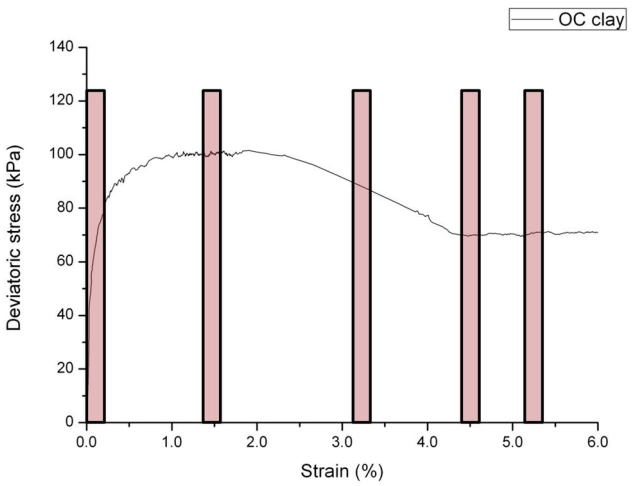


Fig. 3.12 Five stages for digital image analysis

.

By the Chapter 3.3.1 pixel subset size was determined for 80 by 80 pixels. As pixel subset size becomes larger, the accuracy of the digital image analysis becomes higher. However, little pixel subset size has limitation for measurement of spatial deformation.

For optimal conditions of the digital image analysis, images need to be captured under a small strain interval than 0.5% for better accuracy (Jang, 2010). Therefore, 0.25% global axial strain interval was determined.

To minimize the effect of friction at the boundaries of specimen, the images are analyzed for center part of specimen. As shown in Figure 3.13, 893 (19 x 47) center points in the first image of consecutive images are selected. Each center point provides displacement vector, so 893 displacement vectors at the center points of the pixel subsets.

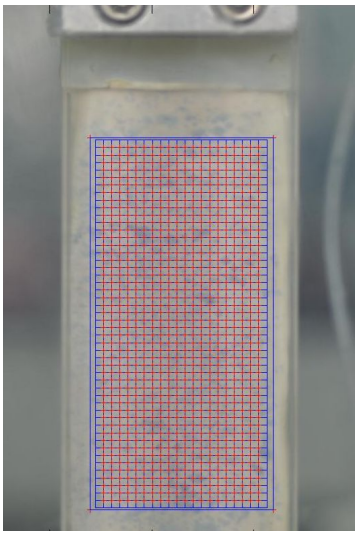

Fig. 3.13 Center points of pixel subsets for displacement computation

# Chapter 4 Experimental Results and Analysis

## 4.1 Introduction

The experimental results of deformation behavior of cohesive soils are accomplished in this chapter. Stress-strain response is evaluated for the result of plane strain test. In addition displacements by the digital image analysis are analyzed and the shear band characteristics also discussed. The topic about deformation characteristics follow the below;

(1) Stress-strain response

(2) Displacement data

(3) Strain distribution

## 4.2 Stress-Strain Response

The stresses and strain are measured by the external load cell transducer and external axial LVDT. The deviator stress and axial strains of NC clay and OC clay are plotted in Figure 4.1 and Figure 4.2.

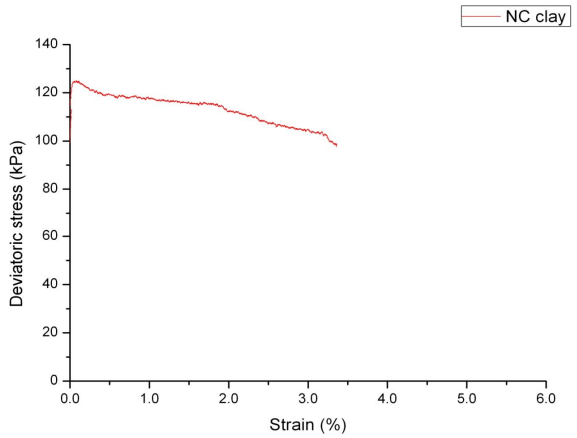


Fig. 4.1 Stress-strain response of NC clay

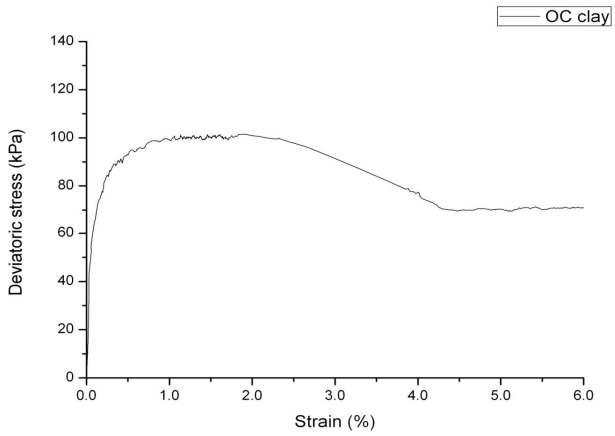


Fig. 4.2 Stress-strain response of OC clay

As shown in Figure 4.1 and Figure 4.2, the strength can be expressed by the effect of consolidation conditions. The strength of NC clay is weaker than the strength of OC clay. Stress reduction phenomenon after a peak stress appears at both soils conditions. However, the stress reduction phenomenon after a peak stress for NC clay appears at smaller strain level than OC clay. The global axial strain at the peak stress is related to over consolidation ratio (OCR).

## 4.3 Displacement Data

Displacement vectors of 893 center point of pixel subset are analyzed by GeoPIV at each stage. In this chapter, the tendencies of displacements during the shear are briefly introduced. The displacement vectors analyzed by GeoPIV and the contours of the displacement are plotted in Figure 4.3 ~ Figure 4.12. The sign of horizontal displacements is positive in right direction, and the sign of axial displacements is positive in downward direction.

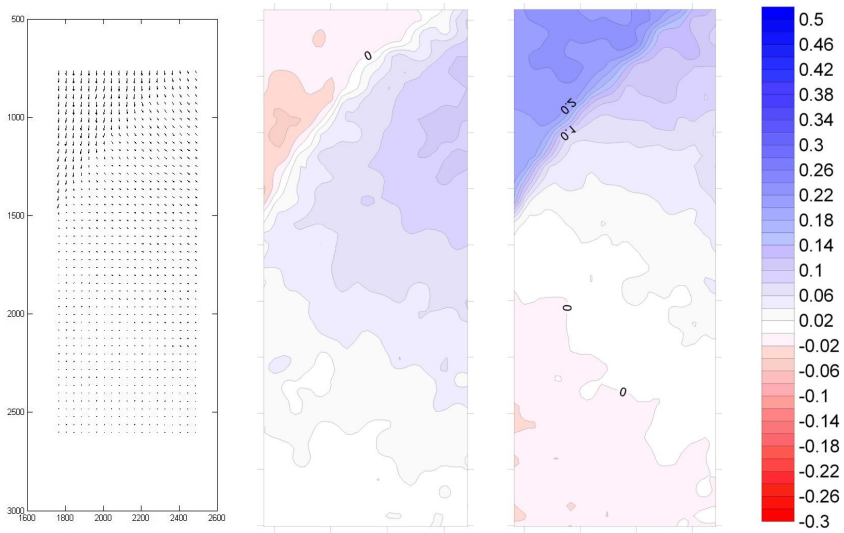


(a) Displacement vector (b) Horizontal contour (c) Vertical contour

Fig. 4.3 Displacement behavior of first stage of NC clay

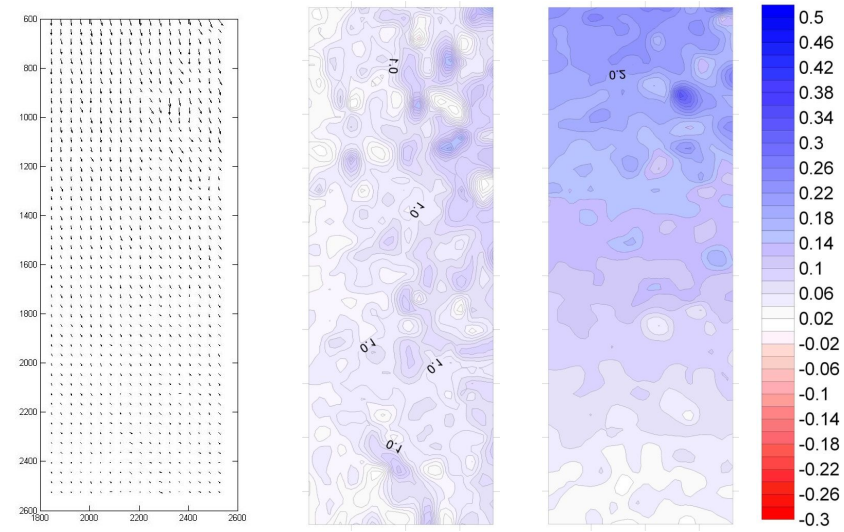


(a) Displacement vector (b) Horizontal contour (c) Vertical contour

Fig. 4.4 Displacement behavior of first stage of OC clay

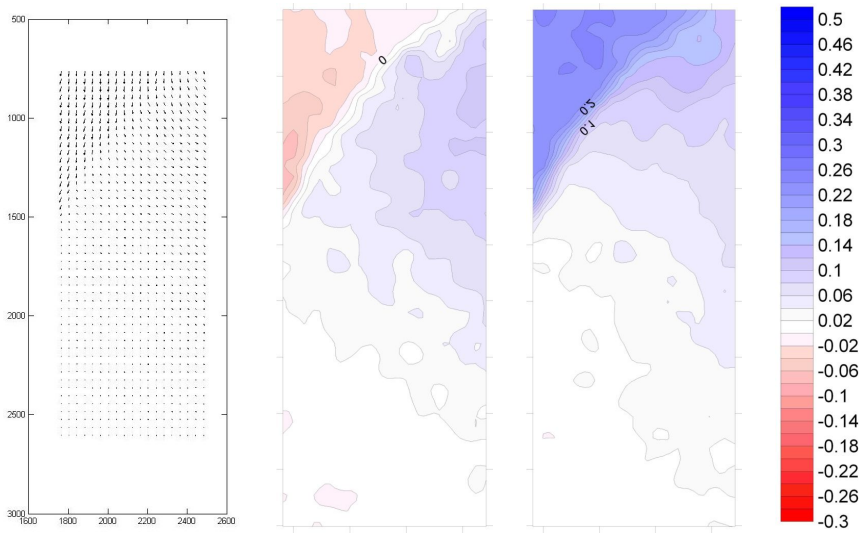


(a) Displacement vector (b) Horizontal contour (c) Vertical contour

Fig. 4.5 Displacement behavior of second stage of NC clay

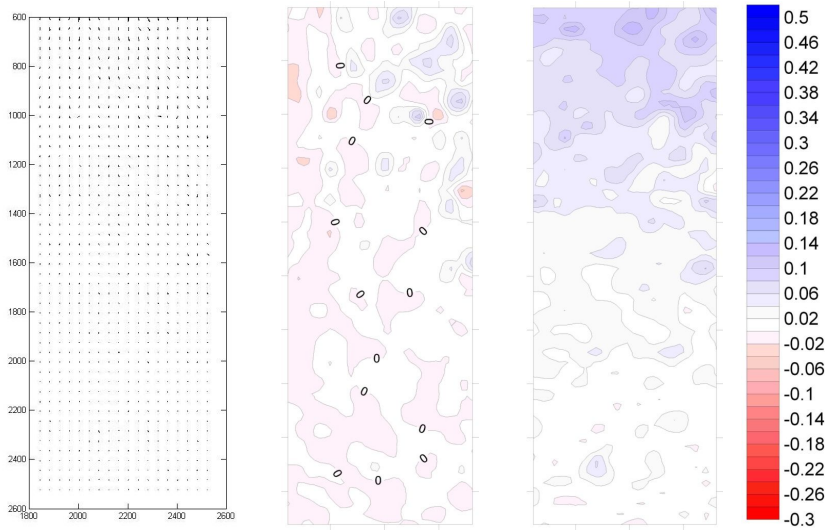


(a) Displacement vector (b) Horizontal contour (c) Vertical contour

Fig. 4.6 Displacement behavior of second stage of OC clay

The first stage for NC clay is peak stage and OC clay is initial stage. As peak stress of NC clay appears at low axial strain level, so that the horizontal and axial displacement tendency is shown distinctly at the first stage. However, the initial stage of OC clay shows relatively heterogeneous displacement. When the specimen reaches the failure including a peak stress state, the contour lines of both horizontal and axial displacement concentrate in a local domain. This displacement concentrated domain can be determined first shear band.

The second stage of NC clay is post peak stage and OC clay is peak stage. After appearance of peak stress at the first stage, the horizontal and axial displacement tendency is clearer than the first stage at NC clay. For OC clay, relatively heterogeneous displacement tendency remains at the second stage. However, little tendency of first shear band appears which can be observed at axial displacement contour.

The third stage of NC clay and OC clay is softening stage. In the softening stage, displacement concentration in a local domain appears distinctly. Double shear band appears at this stage, the first shear band becomes indistinct, and the main shear band appears clearly.

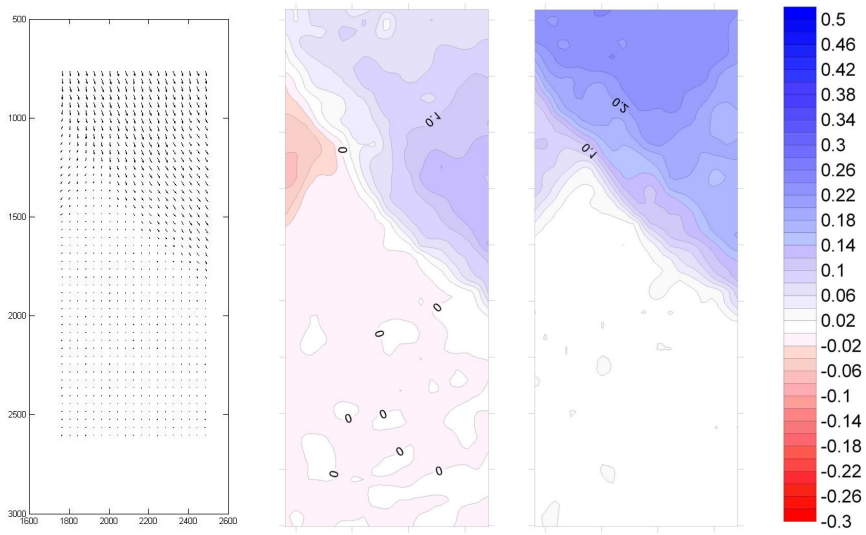


(a) Displacement vector (b) Horizontal contour (c) Vertical contour

Fig. 4.7 Displacement behavior of third stage of NC clay

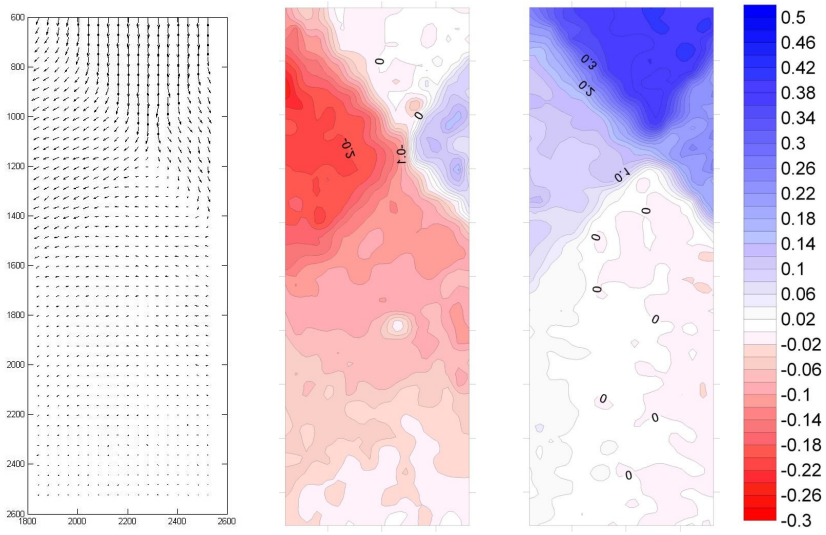


(a) Displacement vector (b) Horizontal contour (c) Vertical contour

Fig. 4.8 Displacement behavior of third stage of OC clay

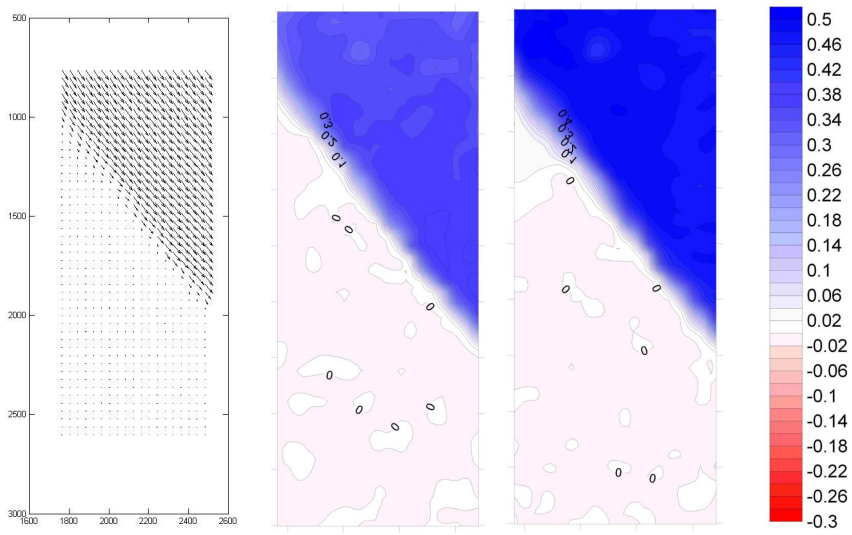


(a) Displacement vector (b) Horizontal contour (c) Vertical contour

Fig. 4.9 Displacement behavior of fourth stage of NC clay

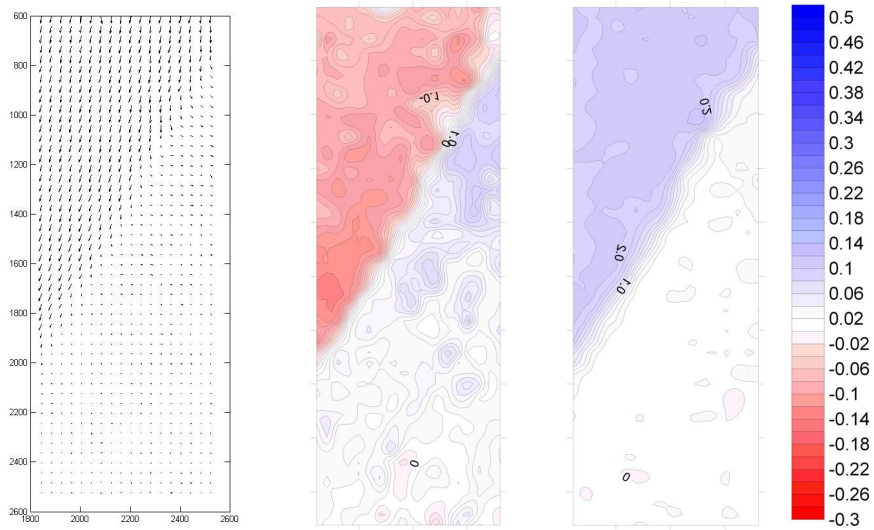


(a) Displacement vector (b) Horizontal contour (c) Vertical contour

Fig. 4.10 Displacement behavior of fourth stage of OC clay

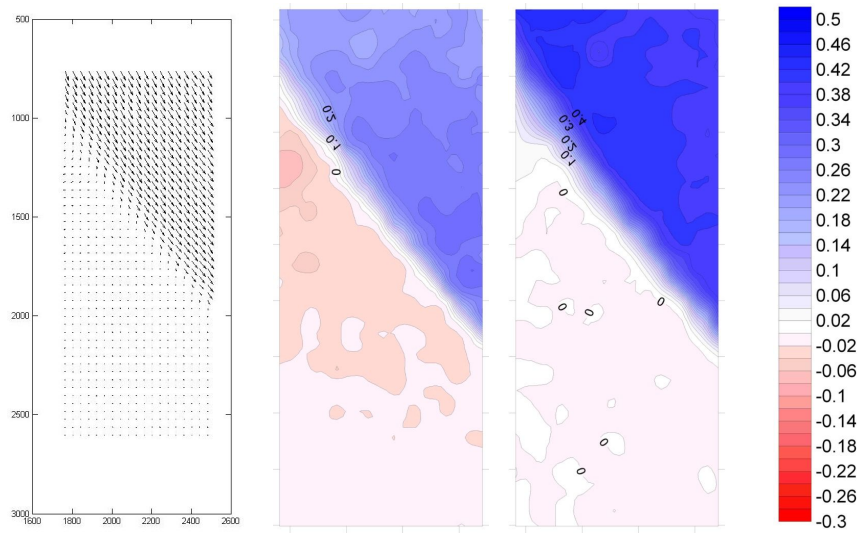


(a) Displacement vector (b) Horizontal contour (c) Vertical contour

Fig. 4.11 Displacement behavior of fifth stage of NC clay

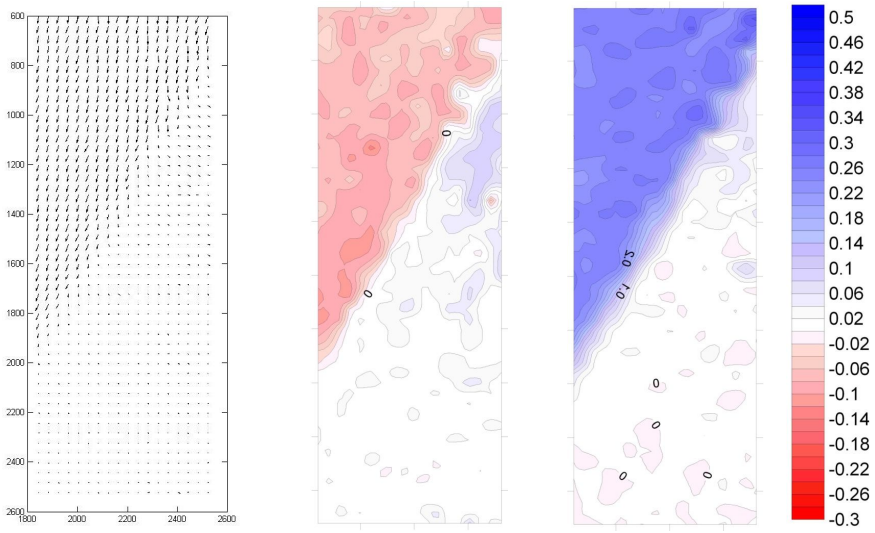


(a) Displacement vector (b) Horizontal contour (c) Vertical contour

Fig. 4.12 Displacement behavior of fifth stage of OC clay

Both of the tested specimens reach a steady state and post failure stage shown in Figure 4.9 ~ Figure 4.12. In these stages definite shear band zone is developed. Displacement concentration near the main shear band is appeared at these stages.

## 4.4 Strain Distribution

Deformation characteristics are evaluated by the concept of the strain which is analyzed from displacement data. Evaluation of strain is analyzed by GeoPIV. Strain distribution is shown in Figure 4.13 ~ Figure 4.17. The magnitude of strain increments is denoted by the color scale. The sign of strain value is defined as blue in lower strain and red in high strain level.

At the first stage, deformation behavior of NC clay and OC clay appears differently. At NC clay, strain concentration appears near the first shear band. However, OC clay shows little tendency of strain concentration.

At the second stage, both of NC clay and OC clay shows the strain concentration near the first shear band. The peak stress of NC clay appears at the first stage, the concentration of deformation appears distinctly in this stage. However the peak stress of OC clay appears at second stage, deformation concentration is appeared indistinctly.

Two shear bands appear at softening stage for both of NC clay and OC clay. Strain concentration is appeared at both shear bands. However strain concentration near the first shear band becomes smaller, and deformation behavior near the main shear band becomes clear.

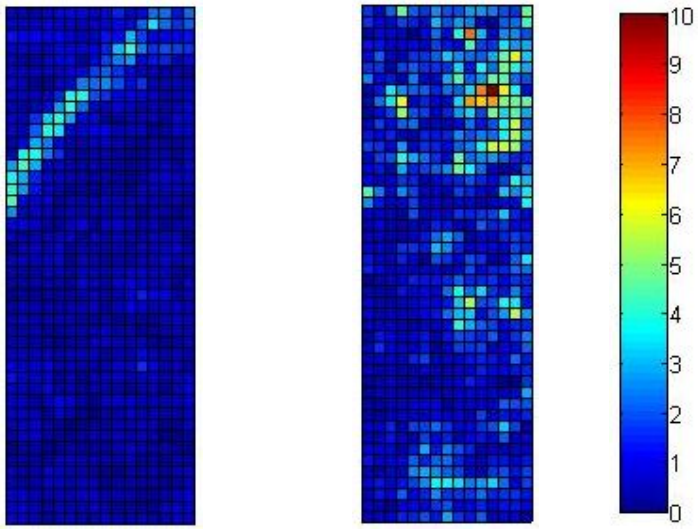


(a) NC clay (b) OC clay

Fig. 4.13 Strain distribution of first stage

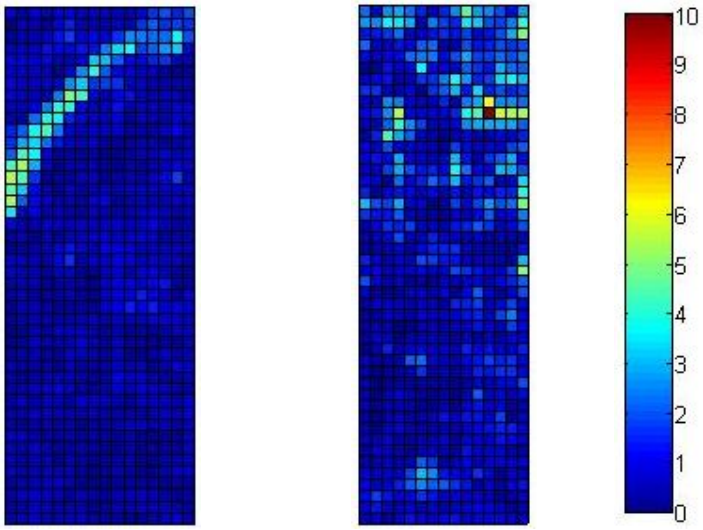


(a) NC clay (b) OC clay

Fig. 4.14 Strain distribution of second stage

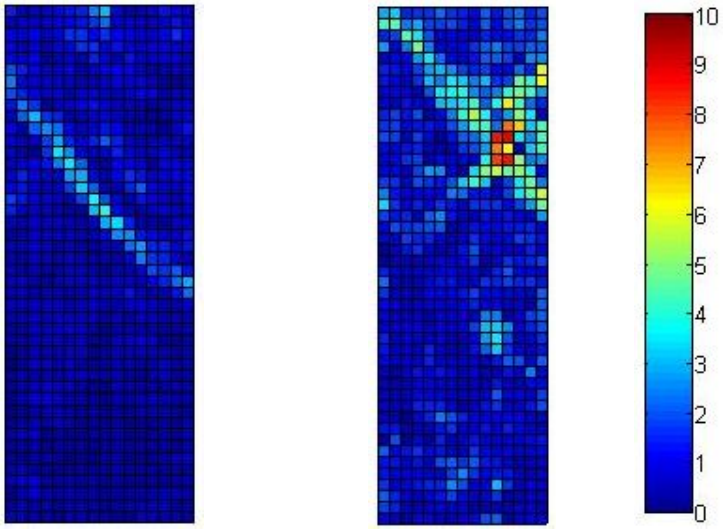


(a) NC clay (b) OC clay

Fig. 4.15 Strain distribution of third stage

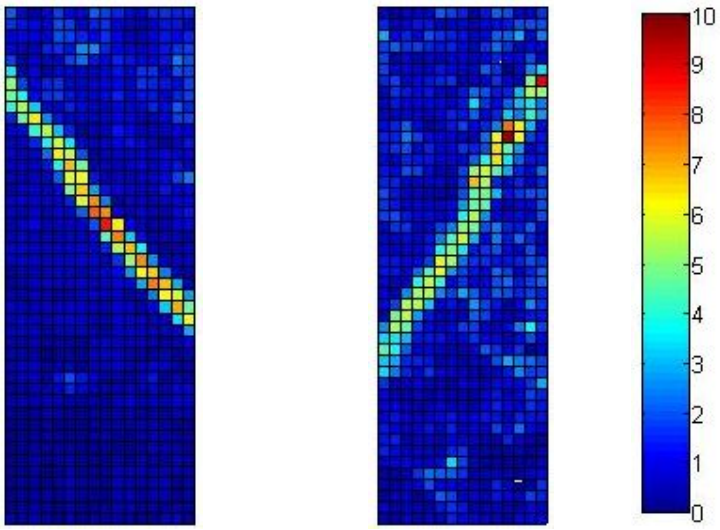


(a) NC clay (b) OC clay

Fig. 4.16 Strain distribution of fourth stage

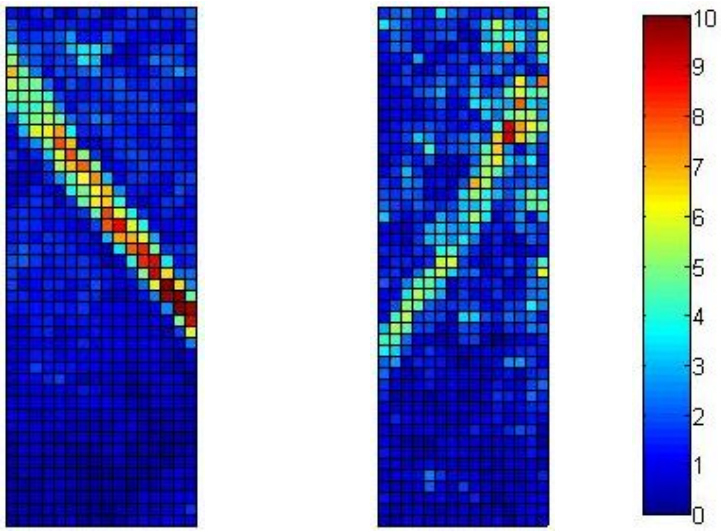


(a) NC clay (b) OC clay

Fig. 4.17 Strain distribution of fifth stage

In the fourth and fifth stage, main shear band appears clearly for both of NC clay and OC clay. In these stages, stain concentration near main shear band appears distinctly. The thickness and inclination weakly increase compare to the softening stage. However, there is no tendency of thickness of shear band affected by consolidation condition. Shear band of OC clay is steeper than that of NC clay. Therefore, it can be determined that shear band inclination has relation with consolidation condition. Thickness and inclination of main shear band is shown in Figure 4.18 and Figure 4.19.

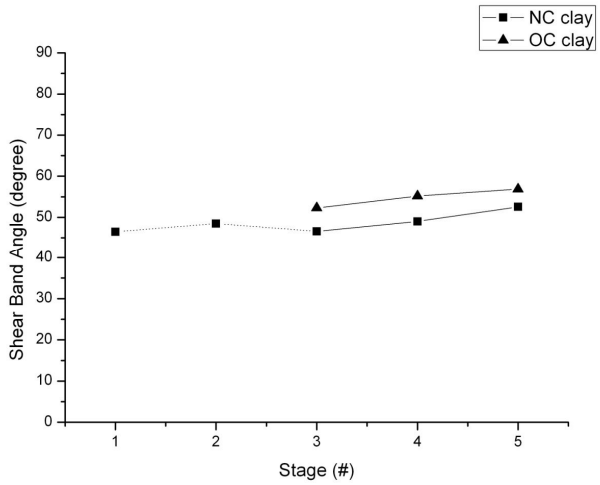


Fig. 4.18 Inclination of shear band

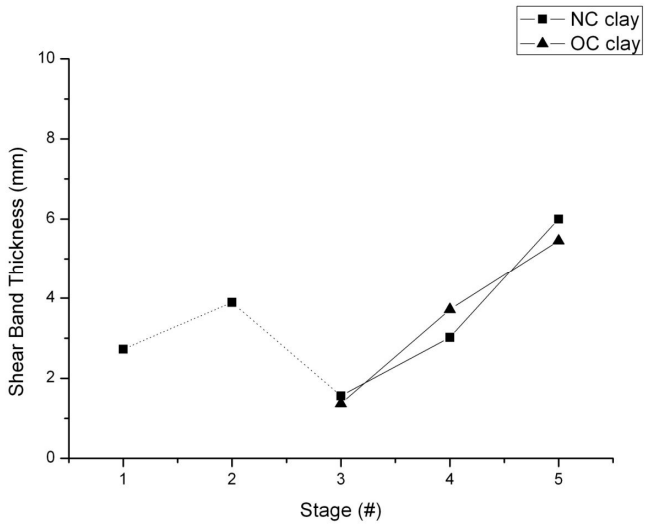


Fig. 4.19 Thickness of shear band

# Chapter 5 Conclusions

Plane strain tests are performed to observe the development of shear band and evaluate the deformation behavior near the shear band. In addition, evaluation of spatial deformation is analyzed by digital image analysis method. Stress-strain behavior is evaluated by the result of plane strain test and displacement and deformation behavior is analyzed. Based on the results and analysis, the following conclusion is determined:

1. Development of shear band has close relation with the peak stress. Peak stress of the cohesive appears at smaller strain level in NC clay than OC clay. In addition soil failure analyzed by digital image analysis, failure occurs faster at NC clay than OC clay.

2. Development of shear band becomes clear in softening stage. At the both of NC clay and OC clay, main shear band appears in softening stage. Though first shear band appears in peak stage; distinct development of first shear band at NC clay, indistinct development of first shear band at OC clay, main shear band appears clearly in softening stage. And then, main shear band is developed in steady state stage.

3. Shear zone has close relation with the strain concentration. Shape of shear band observed by the transparent side wall is similar to the shape of strain concentration zone.

4. For cohesive soil, shear band inclination becomes steeper as shear band is developed. In addition, shear band thickness also becomes larger with the development of shear band.

# Bibliography

김준영, 장의룡, 정충기 (2011), “흙의 변형 측정을 위한 디지털 이미지 해석 기법의 최적화 및 정확도 평가”, 한국지반공학회 논문집, 제 27권, 7호, pp. 5-16.

장의룡, 추윤식, 이원택, 정충기, (2008), “디지털 이미지 코릴레이션 기법으로 평가한 평면변형률 시험의 단부 구속 효과”, 한국지반공학회 논문집, 제24권, 제7호, pp.25-36.

장의룡, 정영훈, 김준영, 정충기, (2011), “평면변형률 시험에서 이미지 해석을 통한 사질토의 전단면 특성 평가”, 한국지반공학회 논문집, 제27권, 제4호, pp.51-65.

Adrian, R. J. (1991), “Particle imaging techniques for experimental fluid mechanics”, Ann. Rev. Fluid Mech, 23, pp.261-304.

Alshibli, K. A., Sture, S. (1999), “Sand Shear Band Thickness Measurements by Digital Imaging Techniques”, Journal of Computing in Civil Engineering, Vol.13, No.2, pp.103-109.

Alshibli, K. A., Sture, S., Costes, N. C., Frank, M. L., Lankton, F. R., Batiste, S. N., and Swanson, R. A. (2000), “Assessment of Localized Deformations in Sand Using X-Ray Computed Tomography”, Geotechnical Testing Journal, Vol.23, No.3, pp.274-299.

Alshibli, K. A., Batiste, S. N., and Sture, S. (2003), “Strain Localization in Sand: Plane Strain vs. Triaxial Compression”, ASCE, Journal of Geotechnical & Geoenvironmental Engineering, Vol.129, No.6, pp.1-12.

Desrues, J.R., Chambon, M.,Mokni, and Mazerolle, F. (1996), “Void Ratio Evolution Inside Shear Bands in Triaxial Sand Specimens Studied by Computed Tomography”, Geotechnique, Vol.46, No.3, pp.529-546.

Finno, R. J., Harris, W. W., Mooney, M. A., and Viggiani, G. (1997), “Shear Bands in Plane Strain Compression of Loose sand”, Geotechnique, Vol.47, No.1, pp.149-165.

Leung, C. F., Xie, Y., Chow, Y. K. (2008), “Use of PIV to Investigate Spudcan-Pile Interaction”, Proc. of the 18th International Offshore and Polar Engineering Conference Vancouver, BC, Canada, pp.721-726.

Liang, L., Saada, A., Figueroa, J. L., and Cope, C.T. (1997), “The Use of Digital Image Processing in Monitoring Shear Band Development”, Geotechnical Testing Journal, Vol.20, No.3, pp.324-339.

Rechenmacher, A. L., and Finno, J. F. (2004), “Digital Image Correlation to Evaluate Shear Banding in Dilative Sands”, Geotechnical Testing Journal, Vol.27, No.1, pp.1-10.

Roscoe, K. H. (1970), “The influence of strains in soil mechanics”, Geotechnique, 20(2), pp.129-170

Vendroux, G., Knauss, W. G. (1998), “Submicron Deformation Field Measurements: Part2. Improved Digital Image Correlation”, Experimental Mechanics, Vol.38, No.2, pp.86-92.

Wong, R. C. K. (2000), “Shear Deformation of locked Sand in Triaxial Compression”, Geotechnical Testing Journal, GTJODJ, Vol.23, No.2, pp.158-170.

White, D. J., Take, W. A., and Bolton, M. D. (2003), “Soil Deformation measurement using particle image velocimetry (PIV) and photogrammetry”, Geotechnique 53, No.7, pp.619-631.

# 초 록

일반적인 흙의 파괴와 깊은 연관이 있는 지반의 압밀 거동에 따른 침하와 전단면의 형성 및 전단면 부근에서의 변형은 지반 구조물의 거동과 안전성에 크게 영향을 미치기 때문에 이에 대한 특성을 파악하는 것이 매우 중요하다. 축대칭 조건인 삼축 시험보다 평면변형률 시험에서 흙의 내부 거동이 더 명확히 관찰되기 때문에 본 연구에서는 평면변형률 조건에서 시험을 진행하여 흙의 압밀 거동 및 전단 거동을 분석하고자 한다. 본 연구에서는 점성토에 대해 이방 압밀을 수행하였다. 이를 위해 재성형된 카올라나이트를 이용하여 압밀을 수행하여 정규압밀 상태와 과압밀 상태로 만들었으며, 이에 대해 전단을 수행하여 전단면의 형성에 대해 관찰하여 비교 및 분석을 수행하였다.

기존의 흙의 압밀 거동 및 전단 거동을 분석하기 위한 방법은 LVDT 등과 같은 계측기를 이용한 전체적인 변위 측정에 따른 분석이 주를 이루었다. 그러나 이런 방법들의 경우 흙의 전체적인 변위는 분석이 가능하나, 흙의 내부에서의 거동에 대한 평가가 불가능하다는 문제점이 있다. 이에 따라서 본 연구에서는 이러한 문제점을 보완하고자 디지털 이미지 해석 기법을 적용하였다. 압밀 과정 및 전단 과정 간 이미지를 촬영하였으며, 취득된 이미지를

통하여 내부의 여러 점에서의 변위에 대해 분석하여 내부 변형에 대한 거동을 평가하였다. 평가된 내부 거동을 통해서 흙의 압밀 조건과 내부 거동에 대한 연관성에 대해 비교 및 분석을 수행하였다.

**주요어 : 평면변형률 시험, 디지털 이미지 해석, 내부 변위 및 변형**

**학 번 : 2012-20891**

# 감사의 글

2012년에 부푼 꿈을 안고 지반연구실에 입학한지 어느새 2년이란 시간이 흘렀습니다. 연구실에 들어와서 처음에는 연구를 잘할 수 있을까 하는 걱정도 많았는데 어느새 석사 학위를 받게 되었습니다. 이렇게 제가 석사 학위를 받을 수 있게 항상 많은 지도를 해주신 교수님들께 감사함니다.

연구에 대한 열정이 넘치시고 항상 올바른 방향으로 갈수 있도록 이끌어주시는 저의 지도교수님이신 정충기 교수님. 처음 연구에 대한 방향부터 마지막 시험이 잘되지 않아 문제가 생겼을 때까지 항상 격려해주시고 잘못된 점은 지적도 많이 해주셔서 많은 가르침을 받을 수 있었습니다. 연구뿐만 아니라 인생에 있어서도 고민이 있을 때마다 조언을 해주시면서 더 큰 그림을 그릴 수 있도록 지도해주셔서 감사합니다. 앞으로 박사과정에 진입을 해서도 교수님께 더 많은 지도를 받아 더 크게 발전할 수 있도록 노력하겠습니다.

카리스마 넘치시면서도 항상 연구실을 생각해주시는 김명모 교수님. 학부 때 가장 먼저 들었던 지반공학 관련 수업인 토질역학 수업에서 느꼈던 지반공학에 대한 흥미가 지반연구실에서 연구를 하게 된 것이 아닌가 생각됩니다. 엄격해 보이시면서도 자상하게 챙겨주셔서 감사합니다.

유머러스 하시면서도 창의적인 발상이 인상적이신 박준범 교수님. 대학원 수업을 들으며 발표를 많이 하면서 발표에 대한 스킬도 배울 수 있었습니다. 교수님처럼 창의적인 생각을 하면서 더 많이 생각할 수 있는 사람이 되도록 하겠습니다.

저에게 많은 도움을 주신 선배님들도 감사합니다. 우선 저의 시험 사수이신 윤식이형. 형님 아니었으면 이 연구가 이루어질 수 있었을까 하는 생각이 듭니다. 학교에 있으실 때도 항상 많이 도와주시고 취직하고 학교를 나가셨는데도 자꾸 문제가 생겨 전화도 드리고 했는데 죄송하고 또 감사합니다. 저의 해석 사수이신 준영이형. 학부 졸업 논문 쓰고 처음 입학했을 때만 해도 정말 무서운 형님이었는데 지금은 형님과 친하게 지내서 좋은거 같습니다. 마지막에 급하게 시험을 마무리하고 해석을 수행할 때 많은 도움을 주셔서 감사합니다. 항상 밤늦게까지 열심히 연구하시는 한샘이형. 형님과 1년과 같은 방을 쓰면서 모르는 것이 있어서 물어볼 때마다 친절히 알려주셔서 감사합니다. 그리고 형수님이 생기셔야 집에 들어갈거 같으니 얼른 결혼하세요! 그래야 형님 건강도 챙기실 수 있습니다. 최근에 결혼하신 가현 누나. 처음 연구실에 입학했을 때는 누나의 술 취한 모습에 놀랐는데 처음 수업 조교를 하면서 궁금한 점이나 문제풀이에 대한 질문을 할때마다 잘 알려주셔서 또 놀랐습니다. 저를 유난히 아껴주셨던 민택이형. 지금은 미국에 나가있지만 조만간 결혼하러 한국에 들어오신다고 하시는데 얼른 결혼하세요. 형님의 화려했던 과거는 형수님 앞에서는 조용히 묻어두겠습니다. 지금은 미국에 계신 석형이형, 인우형. 항상 귀엽게 봐주시고 잘 챙겨주셔서 감사합니다. 한국에 들어오시면 또 한번 뭉쳐봐요. 이번에 박사 학위를 받고 나가시는 선용이형. 형님과 함께 했던 월요회는 진짜 기억에 많이 남을거 같아요. 다른 말도 쓰고 싶지만 여기에는 안 쓰도록 하겠습니다. 저의 첫 방장님이자 지금 방장님인 석중이형. 처음에 형님과 같은 방을 썼던 것이 저의 연구실 적응에 큰 도움이 되지 않았나 싶습니다. 항상 이상한 애교도 부리시지만 형님 덕분에

유쾌한 연구실 생활을 할 수 있었습니다. 새해에는 꼭 모든 일이 잘 되셨으면 좋겠습니다. 특유의 손짓이 인상적이었던 현진이형. 형님과는 자주 술 마시지 못했던거 같아서 아쉽습니다. 바쁘신데도 항상 잘 챙겨주셔서 감사합니다. 2년 동안 파견 나갔다가 돌아오신 희수형. 형과는 석사과정 동안 많이 보지 못해서 아쉬웠습니다. 이제 돌아오셨으니 같이 연구실 생활 재미있게 할 수 있었으면 좋겠습니다. 그리고 13학번 1학기 후배 상래. 처음 봤을 때 참 이런 캐릭터도 있구나 했는데 덕분에 많이 웃었던 것 같다. 급작스럽게 바빠진 이후로 고생이 많은거 같은데 열심히 해라. 그리고 항상 실험 때마다 도와준 정준이. 진짜 많이 실패도 같이 하고 했는데 이제는 다른 길을 가게 되었구나. 그래도 좀 도와주고 그래. 술을 어마어마하게 마시는 슬기. 은수의 빈자리를 채워주나 했는데 파견을 가게 되어 아쉽네. 가서도 열심히 하고 자주 놀러와.

즐거운 대학원 생활을 할 수 있게 해준 06학번 동기들! 언제나 힘들 때마다 도와주고 같이 고민해줘서 고맙다. 연예인 닮은 연구실 선배 성하. 처음 들어왔을 때 같은 방을 너와 함께 쓸 수 있었던 것이 참 즐거웠다. 실험도 같이 하고 삽질도 많이 했는데 앞으로도 열심히 하자. 우린 아직 갈 길이 머니까... 유일한 연구실 동기였던 은수. 학부 때는 아예 모르고 지냈었는데 연구실 와서 친하게 지낼 수 있어서 좋았다. 연구실 와서는 항상 같은 길을 걸어왔는데 이제 너가 나간다니 뭔가 아쉽다. 스크맨이 되었지만 가서도 넌 잘할 수 있을거라 생각한다. 다음은 13학번 1학기 연구실 후배인 통뚱이 승환이. 학부 때부터 알았지만 왠지 덩치에서 패기가 눌려 친하게 지내지 못했었는데 연구실 와서 많이 친해질 수 있어서 좋았다. 평소에 내가 장난도 많이 치고 하는데 선배니까 그런거라고 생각해라. 여자를 정말 좋아하는 종찬이. 실제로 나보다 형이지만

어쩌다 보니 친구가 됐는데 그래서 더 친해질 수 있었던 것 같다. 항상 열심히 노력하는 모습이 인상 깊었어. 열심히 하는 만큼 남은 한학기 열심히 해서 취직 잘해라. 큰 목소리가 인상적이었던 양덕이. 처음에 모르는 얼굴이길래 누나인줄 알고 존댓말 했는데 동기여서 놀랐었어. 얼른 취직 잘되서 참치 한번 사줘. 나의 연구실 선배 지영이. 술자리에서 많이 놀렸는데 미안하고 얼른 취직 잘됐으면 좋겠다.

이외에도 언급하지는 못했지만 이 글을 읽고 계시는 항상 저를 걱정해주시고 아껴주시는 모든 분들께 감사합니다. 더욱더 열심히 노력하여 더 발전하는 사람이 될 수 있도록 노력하겠습니다. 마지막으로 누구보다도 저를 걱정해주시면서도 제가 가는 이 길을 응원해주시는 부모님께 가장 사랑하고 또 감사하다는 말을 전하고 싶습니다.